TECHNISCHE UNIVERSITÄT CHEMNITZ

G. Of G. J. Rodin O. Steinbach M. Taus

Coupling Methods for Interior Penalty Discontinuous Galerkin Finite Element Methods and Boundary Element Methods

CSC/11-02

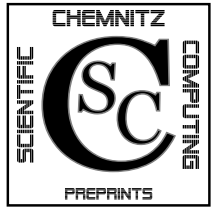

Chemnitz Scientific Computing Preprints

Chemnitz Scientific Computing Preprints – ISSN 1864-0087

and so

$$
\begin{aligned}
c_1^{\mathcal{A}} \|(u_{i,h} - v_h, u_{e,h} - q_h)\|_{\mathcal{A}} \;&\leq \\
&\leq c \Big[\|(S^{\text{ext}} - \widetilde{S}) u_e\|^2_{H^{-1/2}(\Gamma)} + \|u_e - q_h\|^2_{H^{1/2}(\Gamma)} + \|u_i - v_h\|^2_{DG} \\
&\quad + \sum_{e \in \mathcal{E}_h^{\text{ext}}} h_e \|n \cdot \nabla (u_i - v_h)\|^2_{L^2(e)} + \sum_{e \in \mathcal{E}_h^{\text{ext}}} \frac{1 + \sigma_e}{h_e} \|(u_i - v_h) - (u_e - q_h)\|^2_{L^2(e)} \Big]^{1/2} .
\end{aligned}
$$

This inequality implies the error estimate given in Theorem 4.3.

Impressum:

Chemnitz Scientific Computing Preprints — ISSN 1864-0087
(1995–2005: Preprintreihe des Chemnitzer SFB393)

Herausgeber:
Professuren für
Numerische und Angewandte Mathematik
an der Fakultät für Mathematik
der Technischen Universität Chemnitz

Postanschrift:
TU Chemnitz, Fakultät für Mathematik
09107 Chemnitz
Sitz:
Reichenhainer Str. 41, 09126 Chemnitz

http://www.tu-chemnitz.de/mathematik/csc/

$$
\begin{aligned}
\leq\ & \|(S^{\rm ext}-\widetilde{S})u_e\|_{H^{-1/2}(\Gamma)}\|u_{e,h}-q_h\|_{H^{1/2}(\Gamma)} + c_2^{\widetilde{S}}\|u_e-q_h\|_{H^{1/2}(\Gamma)}\|u_{e,h}-q_h\|_{H^{1/2}(\Gamma)} \\
& + c_2^{\mathcal{A}}\|u_i-v_h\|_{DG}\|u_{i,h}-v_h\|_{DG} \\
& + \sum_{e\in\mathcal{E}_h^{\rm ext}} \|n\cdot\nabla(u_i-v_h)\|_{L^2(e)}\|(u_{i,h}-v_h)-(u_{e,h}-q_h)\|_{L^2(e)} \\
& + \sum_{e\in\mathcal{E}_h^{\rm ext}} \|n\cdot\nabla(u_{i,h}-v_h)\|_{L^2(e)}\|(u_i-v_h)-(u_e-q_h)\|_{L^2(e)} \\
& + \sum_{e\in\mathcal{E}_h^{\rm ext}} \frac{\sigma_e}{h_e}\|(u_i-v_h)-(u_e-q_h)\|_{L^2(e)}\|(u_{i,h}-v_h)-(u_{e,h}-q_h)\|_{L^2(e)}.
\end{aligned}
$$

By applying the weighted Hölder inequality we obtain

$$
\begin{aligned}
c_1^{\mathcal{A}}\|(u_{i,h}-v_h,u_{e,h}-q_h)\|_{\mathcal{A}}^2 \ \leq\ & \\
\leq c\ \Bigg[& \|(S^{\rm ext}-\widetilde{S})u_e\|_{H^{-1/2}(\Gamma)}^2 + \|u_e-q_h\|_{H^{1/2}(\Gamma)}^2 + \|u_i-v_h\|_{DG}^2 \\
& + \sum_{e\in\mathcal{E}_h^{\rm ext}} h_e\|n\cdot\nabla(u_i-v_h)\|_{L^2(e)}^2 + \sum_{e\in\mathcal{E}_h^{\rm ext}} \frac{1+\sigma_e}{h_e}\|(u_i-v_h)-(u_e-q_h)\|_{L^2(e)}^2\Bigg]^{1/2} \\
\cdot\ \Bigg[& \|u_{e,h}-q_h\|_{H^{1/2}(\Gamma)}^2 + \|u_{i,h}-v_h\|_{DG}^2 + \sum_{e\in\mathcal{E}_h^{\rm ext}} h_e\|n\cdot\nabla(u_{i,h}-v_h)\|_{L^2(e)}^2 \\
& + \sum_{e\in\mathcal{E}_h^{\rm ext}} \frac{1+\sigma_e}{h_e}\|(u_{i,h}-v_h)-(u_{e,h}-q_h)\|_{L^2(e)}^2\Bigg]^{1/2}.
\end{aligned}
$$

Let $T_e\in\mathcal{T}_h$ be a finite element containing a face $e\in\mathcal{E}_h^{\rm ext}$. Then for a finite element function $v_h\in\mathcal{V}_h$ we obtain

$$
\|n\cdot\nabla v_h\|_{L^2(e)} \ \leq\ c\,h_e^{-1/2}\|\nabla v_h\|_{L^2(T_e)},
$$

and

$$
\sum_{e\in\mathcal{E}_h^{\rm ext}} h_e\|n\cdot\nabla(u_{i,h}-v_h)\|_{L^2(e)}^2 \ \leq\ c\sum_{T\in\mathcal{T}_h}\|\nabla(u_{i,h}-v_h)\|_{L^2(T)}^2.
$$

Hence we obtain

$$
\begin{aligned}
\Bigg[& \|u_{e,h}-q_h\|_{H^{1/2}(\Gamma)}^2 + \|u_{i,h}-v_h\|_{DG}^2 + \sum_{e\in\mathcal{E}_h^{\rm ext}} h_e\|n\cdot\nabla(u_{i,h}-v_h)\|_{L^2(e)}^2 \\
& + \sum_{e\in\mathcal{E}_h^{\rm ext}} \frac{1+\sigma_e}{h_e}\|(u_{i,h}-v_h)-(u_{e,h}-q_h)\|_{L^2(e)}^2\Bigg]^{1/2} \leq c\,\|(u_{i,h}-v_h,u_{e,h}-q_h)\|_{\mathcal{A}},
\end{aligned}
$$

TECHNISCHE UNIVERSITÄT CHEMNITZ

Chemnitz Scientific Computing Preprints

G. Of G. J. Rodin O. Steinbach M. Taus

Coupling Methods for Interior Penalty Discontinuous Galerkin Finite Element Methods and Boundary Element Methods

CSC/11-02

Abstract

This paper presents three new coupling methods for interior penalty discontinuous Galerkin finite element methods and boundary element methods. The new methods allow one to use discontinuous basis functions on the interface between the subdomains represented by the finite element and boundary element methods. This feature is particularly important when discontinuous Galerkin finite element methods are used. Error and stability analysis is presented for some of the methods. Numerical examples suggest that all three methods exhibit very similar convergence properties, consistent with available theoretical results.

CSC/11-02 ISSN 1864-0087 **September 2011**

Contents

1. Introduction 1

2. Model Problem and Background 2
   2.1. Boundary Integral Equations . . . 2
   2.2. Interior Penalty DG Finite Element Methods . . . 4
   2.3. Coupling Methods . . . 5

3. New Coupling Methods 7
   3.1. First Method: Non–Symmetric Coupling . . . 7
   3.2. Second Method: Symmetric Three–Field Approach . . . 9
   3.3. Third Method: Dirichlet Based Coupling . . . 10

4. Stability and Error Analysis 12

5. Numerical Examples 16

6. Summary 18

A. Appendix 21

Author's addresses:

Günter Of
Fakultät für Mathematik, Technische Universität Chemnitz, Reichenhainer Str. 41, 09126 Chemnitz, Germany. of@tugraz.at

Olaf Steinbach
Institut für Numerische Mathematik, Technische Universität Graz, Steyrergasse 30, 8010 Graz, Austria. o.steinbach@tugraz.at

Gregory J. Rodin
Institute for Computational Engineering and Sciences, The University of Texas at Austin, Austin, TX, 78712, USA. gjr@ices.utexas.edu

Matthias Taus
Institute for Computational Engineering and Sciences, The University of Texas at Austin, Austin, TX, 78712, USA. taus@ices.utexas.edu

[26] W. L. Wendland: On asymptotic error estimates for the combined BEM an FEM. In: In Finite Element and Boundary Element Techniques from Mathematical and Engineering Point of View (E. Stein, W. L. Wendland eds.), CISM Lecture Notes, vol. 301, Springer, Wien, pp. 273–333, 1988.

[27] M. F. Wheeler: An elliptic collocation–finite element method with interior penalties. SIAM J. Numer. Anal. 15 (1978) 152–161.

A. Appendix

In this appendix we prove the error estimate given in Theorem 4.3. For arbitrary $(v_h, q_h) \in \mathcal{V}_h \times \mathcal{Q}_h$, the triangle inequality implies

$$\|(u_i - u_{i,h}, u_e - u_{e,h})\|_{\mathcal{A}} \leq \|(u_i - v_h, u_e - q_h)\|_{\mathcal{A}} + \|(u_{i,h} - v_h, u_{e,h} - q_h)\|_{\mathcal{A}}.$$

The first term can be further estimated by using standard techniques, hence it remains to bound the second term. We use the ellipticity estimate (4.4) and the perturbed Galerkin orthogonality (4.6) to obtain

$$\begin{aligned} c_1^{\mathcal{A}}\|(u_{i,h} - v_h, u_{e,h} - q_h)\|_{\mathcal{A}}^2 &\leq \mathcal{A}(u_{i,h} - v_h, u_{e,h} - q_h; u_{i,h} - v_h, u_{e,h} - q_h) \\ &= \mathcal{A}(u_{i,h} - u_i, u_{e,h} - u_e; u_{i,h} - v_h, u_{e,h} - q_h) + \mathcal{A}(u_i - v_h, u_e - q_h; u_{i,h} - v_h, u_{e,h} - q_h) \\ &= \langle (S^{\text{ext}} - \widetilde{S})u_e, u_{e,h} - q_h\rangle_\Gamma + \mathcal{A}(u_i - v_h, u_e - q_h; u_{i,h} - v_h, u_{e,h} - q_h). \end{aligned}$$

By combining this equation with (4.1) we obtain

$$\begin{aligned} &c_1^{\mathcal{A}}\|(u_{i,h} - v_h, u_{e,h} - q_h)\|_{\mathcal{A}}^2 \\ &\leq \langle (S^{\text{ext}} - \widetilde{S})u_e, u_{e,h} - q_h\rangle_\Gamma + \mathcal{A}(u_i - v_h, u_e - q_h; u_{i,h} - v_h, u_{e,h} - q_h) \\ &= \langle (S^{\text{ext}} - \widetilde{S})u_e, u_{e,h} - q_h\rangle_\Gamma + \langle \widetilde{S}(u_e - q_h), u_{e,h} - q_h\rangle_\Gamma + a_{DG}(u_i - v_h, u_{i,h} - v_h) \\ &\quad - \langle n \cdot \nabla(u_i - v_h), (u_{i,h} - v_h) - (u_{e,h} - q_h)\rangle_\Gamma + \eta\langle n \cdot \nabla(u_{i,h} - v_h), (u_i - v_h) - (u_e - q_h)\rangle_\Gamma \\ &\quad + \sum_{e \in \mathcal{E}_h^{\text{ext}}} \frac{\sigma_e}{h_e} \int_e [(u_i - v_h) - (u_e - q_h)][(u_{i,h} - v_h) - (u_{e,h} - q_h)] ds_x \end{aligned}$$

[11] G. C. Hsiao, E. Schnack, W. L. Wendland: Hybrid coupled finite–boundary element methods for elliptic systems of second order. Comput. Methods Appl. Mech. Engrg. 190 (2000) 431–485.

[12] G. C. Hsiao, W. L. Wendland: Boundary integral equations. Applied Mathematical Sciences, vol. 164, Springer, Berlin, 2008.

[13] C. Johnson, J.–C. Nédélec: On the coupling of boundary integral and finite element methods. Math. Comp. 35 (1980) 1063–1079.

[14] W. McLean: Strongly Elliptic Systems and Boundary Integral Equations. Cambridge University Press, 2000.

[15] J.–C. Nédélec: Curved finite element methods for the solution of singular integral equations on surfaces in $\mathbb{R}^3$. Comp. Meth. Appl. Mech. Engrg. 8 (1976) 61–80.

[16] J.–C. Nédélec: Integral equations with nonintegrable kernels. Int. Eq. Operator Th. 5 (1982) 562–572.

[17] G. Of, O. Steinbach: A fast multipole boundary element method for a modified hypersingular boundary integral equation. In: Analysis and Simulation of Multifield Problems (M. Efendiev, W. L. Wendland eds.), Lecture Notes in Applied and Computational Mechanics, vol. 12, Springer, Berlin, pp. 163–169, 2003.

[18] G. Of, O. Steinbach, W. L. Wendland: The fast multipole method for the symmetric boundary integral formulation. IMA J. Numer. Anal. 26 (2006) 272–296.

[19] B. Rivière: Discontinuous Galerkin methods for solving elliptic and parabolic equations. Frontiers in Applied Mathematics, vol. 35, SIAM, Philadelphia, 2008.

[20] B. Rivière, M. F. Wheeler, V. Girault: Improved energy estimates for interior penalty, constrained and discontinuous Galerkin methods for elliptic problems. I. Comput. Geosci. 3 (2000) 337–360.

[21] S. A. Sauter, C. Schwab: Boundary Element Methods. Springer Series in Computational Mathematics, vol. 39. Springer, Berlin, 2011.

[22] F.–J. Sayas: The validity of Johnson–Nedelec's BEM–FEM coupling on polygonal interfaces. SIAM J. Numer. Anal. 47 (2009) 3451–3463.

[23] O. Steinbach: Stability estimates for hybrid coupled domain decomposition methods. Lecture Notes in Mathematics, vol. 1809, Springer, Heidelberg, 2003.

[24] O. Steinbach: Numerical Approximation Methods for Elliptic Boundary Value Problems. Finite and Boundary Elements. Springer, New York, 2008.

[25] O. Steinbach: A note on the stable one–equation coupling of finite and boundary elements. SIAM J. Numer. Math. 49 (2011) 1521–1531.

1. Introduction

This paper is concerned with coupling methods for finite element and boundary element methods. Such coupling methods are advantageous for problems whose domain involves an interior finite subdomain(s) embedded in an exterior unbounded subdomain, such that in the interior subdomain the governing partial differential equations are complex and require finite element methods, whereas in the exterior subdomain the governing partial differential equations are simple and can be solved using boundary element methods. The coupling methods are well established in the literature for classical (continuous) finite element and boundary element methods; we refer to [11] and the references given therein.

This paper is motivated by applications that require discontinuous Galerkin (DG) rather than continuous finite element methods. Coupling methods involving DG finite element methods have been analyzed by Bustinza, Gatica, Heuer, and Sayas [2, 3, 8, 9], who established that essentially any boundary element method can be combined with any DG finite element method, as long as one uses approximations continuous on the interface. For two–dimensional problems, this restriction can be removed if one combines DG finite element methods with a particular Galerkin boundary element method [8].

The coupling methods considered by Bustinza, Gatica, Heuer, and Sayas are based on the symmetric formulation of boundary integral equations. In this case, unique solvability of the coupling method is a direct consequence of the unique solvability of the underlying finite element and boundary element systems. A disadvantage of symmetric boundary element methods is that they involve the hypersingular boundary integral operator that not only precludes the use of basic collocation schemes but also requires functions continuous on the interface. The latter restriction is particularly undesirable for coupling methods involving DG finite element methods in $\mathbb{R}^3$ [8].

In this paper, we present three new methods that allow for discontinuous functions on the interface, and therefore significantly simplify the coupling between DG finite element methods with either Galerkin or collocation boundary element methods. The first method is based on the Johnson–Nédélec coupling [13] extended to DG finite element methods. This method admits both collocation and Galerkin boundary element methods. However, the method gives rise to non–symmetric linear algebraic problems and its mathematical foundations have not been established. The second method, which combines a three–field approach [1] and a symmetric boundary integral formulation, addresses some of the drawbacks of the first method, but it involves the hypersingular operator, and therefore it is limited to Galerkin boundary element methods. This method gives rise to non–symmetric but well–structured linear algebraic problems that can be solved almost as efficiently as symmetric ones. Following the coupling approach of DG and mixed finite element methods [10] the third method gives one two options. The first option admits both collocation and Galerkin schemes and results in non–symmetric linear algebraic problems. This option has the advantage of having a sound mathematical foundation for the Galerkin scheme. The second option is limited to Galerkin boundary element methods, but it results in symmetric

linear algebraic problems and has a sound mathematical foundation.

The rest of the paper is organized as follows. In Section 2, we introduce a model problem and briefly outline relevant existing results necessary for presenting the new methods. In Section 3, we present the new coupling methods. In Section 4, we establish unique solvability and error estimates for one of the methods. In Section 5, we present numerical results indicating that the proposed methods and their variants have very similar convergence properties, and those properties are consistent with available theoretical results. The paper is concluded with a brief summary.

2. Model Problem and Background

For a bounded domain $\Omega \subset \mathbb{R}^3$ with a Lipschitz boundary $\Gamma := \partial\Omega$ and a given volume density $f \in L^2(\Omega)$, the model problem involves the partial differential equations

$$-\Delta u_i = f \quad \text{in } \Omega, \quad -\Delta u_e = 0 \quad \text{in } \Omega^c := \mathbb{R}^3 \backslash \overline{\Omega}, \tag{2.1}$$

the transmission conditions

$$[\![u]\!] := u_e - u_i = 0 \quad \text{and} \quad [\![n \cdot \nabla u]\!] = n \cdot (\nabla u_e - \nabla u_i) = 0 \quad \text{on } \Gamma, \tag{2.2}$$

and the radiation condition

$$u_e(x) = \mathcal{O}\left(\frac{1}{|x|}\right) \quad \text{as } |x| \to \infty. \tag{2.3}$$

Here n denotes the outward unit normal vector on Γ.

For our purposes, it is expedient to decouple the stated boundary value problem (2.1)–(2.3) into an interior boundary value problem for the subdomain Ω and an exterior boundary value problem for the subdomain Ω^c. We suppose that the numerical treatment of the interior and exterior problems is based on DG finite element and boundary element methods, respectively. Our objective is to identify appropriate interior and exterior boundary value problems, boundary integral equations for the exterior problems, and discretization schemes on Γ.

2.1. Boundary Integral Equations

The Cauchy data $u_{e|\Gamma}$ and $t_e := (n \cdot \nabla u_e)_{|\Gamma}$ uniquely define a harmonic function $u_e(x)$ for $x \in \Omega^c$ via the representation formula, e.g. [24],

$$u_e(x) = -\int_\Gamma U^*(x,y) t_e(y) ds_y + \int_\Gamma \frac{\partial}{\partial n_y} U^*(x,y) u_e(y) ds_y \,, \tag{2.4}$$

Acknowledgement

The authors would like to thank M. Neumüller for providing the DG solver which was used for the DG part of all computations reported in this paper. GJR acknowledges the financial support from the Department of Energy (grant DOE 06-14-11 DE-FG02-05ER25701) and by the W. A. "Tex" Moncrief, Jr. Endowment In Simulation–Based Engineering Sciences through a Grand Challenge Faculty Fellowship. MT acknowledges the financial support from the Fulbright Foundation.

References

[1] F. Brezzi, L. D. Marini: A three–field domain decomposition method. Contemp. Math. 157 (1994) 27–34.

[2] R. Bustinza, G. N. Gatica, F.–J. Sayas: A LDG–BEM coupling for a class of nonlinear exterior transmission problems. In: Numerical Mathematics and Advanced Applications, Springer, Berlin, pp. 1129–1136, 2006.

[3] R. Bustinza, G. N. Gatica, F.–J. Sayas: On the coupling of local discontinuous Galerkin and boundary element methods for non–linear exterior transmission problems. IMA J. Numer. Anal. 28 (2008) 225–244.

[4] C. Carstensen, M. Maischak, D. Praetorius, E. P. Stephan: Residual–based a posteriori error estimate for hypersingular equation on surfaces. Numer. Math. 97 (2004) 397–425.

[5] P. G. Ciarlet: The Finite Element Method for Elliptic Problems. North–Holland, 1978.

[6] M. Costabel: Symmetric methods for the coupling of finite elements and boundary elements. In: Boundary Elements IX (C. A. Brebbia, G. Kuhn, W. L. Wendland eds.), Springer, Berlin, pp. 411–420, 1987.

[7] M. Costabel: Boundary integral operators on Lipschitz domains: elementary results. SIAM J. Math. Anal. 19 (1988) 613–626.

[8] G. N. Gatica, N. Heuer, F.–J. Sayas: A direct coupling of local discontinuous Galerkin and boundary element methods. Math. Comp. 79 (2010) 1369–1394.

[9] G. N. Gatica, F.–J. Sayas: An a priori error analysis for the coupling of local discontinuous Galerkin and boundary element methods. Math. Comp. 75 (2006) 1675–1696.

[10] V. Girault, S. Sun, M. F. Wheeler, I. Yotov: Coupling discontinuous Galerkin and mixed finite element discretizations using mortar finite elements. SIAM J. Numer. Anal. 46 (2008) 949–979.

			Galerkin (3.10)			
N_Ω	N_Γ	M_Γ	e_{DG}	eoc	e_2	eoc
181	122	63	0.88015		0.152248	
1448	488	246	0.51954	0.76	0.051223	1.57
11584	1952	978	0.29298	0.83	0.016932	1.60
92672	7808	3906	0.15569	0.91	0.004979	1.77
741376	31232	15618	0.07990	0.96	0.001345	1.89

Table 3: Errors and rates of convergence for the second method measured using the energy norm and L_2–norms.

			Galerkin (3.5)				Collocation (3.6)			
N_Ω	N_Γ	M_Γ	e_{DG}	eoc	e_2	eoc	e_{DG}	eoc	e_2	eoc
181	122	63	0.87850		0.15124		0.87541		0.14699	
1448	488	246	0.51920	0.76	0.05100	1.56	0.51871	0.76	0.04980	1.56
11584	1952	978	0.29293	0.83	0.01689	1.59	0.29288	0.82	0.01662	1.58
92672	7808	3906	0.15568	0.91	0.00497	1.76	0.15568	0.91	0.00491	1.76
741376	31232	15618	0.07990	0.96	0.00135	1.88	0.07990	0.96	0.00133	1.88

Table 4: Errors and rates of convergence for the first method measured using the energy norm and L_2–norms.

energy norm and quadratic order of convergence in the $L_2(\Omega)$–norm. Furthermore, the differences in the absolute values of the corresponding errors appear to be minimal.

6. Summary

This paper introduces three new coupling methods for the interior penalty DG finite element methods and boundary element methods. The key advantage of the new methods is that they allow one to use discontinuous basis functions on the interface, which is particularly important for coupling methods involving DG finite element methods. The new coupling methods have six variations associated with different approximations of the Steklov–Poincaré operator of the underlying boundary integral equations. We presented theoretical results pertaining to stability and error analysis for some of the versions of the methods, whereas establishing such results for other versions can be done in a similar way. Numerical results suggest that all versions perform very similar to each other, and exhibit expected rates of convergence in both energy and L_2–norms.

which satisfies the radiation condition (2.3), and where

$$U^*(x,y) = \frac{1}{4\pi}\frac{1}{|x-y|}$$

is the fundamental solution of the Laplace operator.

The Cauchy data $u_{e|\Gamma}$ and t_e can be related to each other using boundary integral equations on Γ, all of which follow from the exterior Calderon projection

$$\begin{pmatrix} u_e \\ t_e \end{pmatrix} = \begin{pmatrix} \frac{1}{2}I + K & -V \\ -D & \frac{1}{2}I - K' \end{pmatrix} \begin{pmatrix} u_e \\ t_e \end{pmatrix}. \tag{2.5}$$

Here for $x \in \Gamma$

$$(Vt_e)(x) = \int_\Gamma U^*(x,y)t_e(y)ds_y, \quad (Ku_e)(x) = \int_\Gamma \frac{\partial}{\partial n_y}U^*(x,y)u_e(y)ds_y,$$

$$(K't_e)(x) = \int_\Gamma \frac{\partial}{\partial n_x}U^*(x,y)t_e(y)ds_y, \quad (Du_e)(x) = -\frac{\partial}{\partial n_x}\int_\Gamma \frac{\partial}{\partial n_y}U^*(x,y)u_e(y)ds_y$$

denote the single layer, double layer, adjoint double layer, and the hypersingular boundary integral operators, respectively. The mapping properties of these operators are well established, e.g. [7, 12, 14, 21, 24]. In particular, the single layer operator $V : H^{-1/2}(\Gamma) \to H^{1/2}(\Gamma)$ is bounded and $H^{-1/2}(\Gamma)$–elliptic, and therefore invertible. Hence equations (2.5) imply the Dirichlet to Neumann map

$$t_e = -V^{-1}(\frac{1}{2}I - K)u_e = -\left[D + (\frac{1}{2}I - K')V^{-1}(\frac{1}{2}I - K)\right]u_e =: -S^{\text{ext}}u_e. \tag{2.6}$$

Let us note that both representations of the Steklov–Poincaré operator $S^{\text{ext}} : H^{1/2}(\Gamma) \to H^{-1/2}(\Gamma)$ are self–adjoint in the continuous setting. However, these representations may have different stability and symmetry properties in the discrete setting, e.g. [23]. Finally, let us mention that the bilinear form induced by the hypersingular operator D allows for an alternative representation that involves weakly singular surface integrals only [16]:

$$\langle Du, v\rangle_\Gamma = \frac{1}{4\pi}\int_\Gamma\int_\Gamma \frac{\underline{\text{curl}}_\Gamma u(y) \cdot \underline{\text{curl}}_\Gamma v(x)}{|x-y|}ds_y ds_x \quad \text{for all } u, v \in H^{1/2}(\Gamma) \cap C(\Gamma), \tag{2.7}$$

where $\underline{\text{curl}}_\Gamma$ is the surface curl operator. This representation is central to Galerkin boundary element methods involving the hypersingular operator D, as it allows one to represent the action of D in terms of the single layer operator V. Let us emphasize that (2.7) holds for continuous densities u and v only; otherwise (2.7) must include additional terms.

2.2. Interior Penalty DG Finite Element Methods

In the proposed coupling methods, DG finite element methods are restricted to interior penalty methods [19, 20, 27] which are well studied and widely applied.

Let $\mathcal{T}_h = \{T_\ell\}_{\ell=1}^{N_\Omega}$ be a finite element mesh of the interior domain Ω. For an element $T \in \mathcal{T}_h$, we identify the boundary ∂T, the diameter h_T, and the outward unit normal vector n_T. We define the global mesh size $h := \max_{T\in\mathcal{T}_h} h_T$. The interior and exterior element faces of the finite element mesh are defined as

$$\mathcal{E}_h^{\text{int}} := \{e : \exists T_\alpha, T_\beta \in \mathcal{T}_h : e = \partial T_\alpha \cap \partial T_\beta, \alpha \neq \beta\},$$

and

$$\mathcal{E}_h^{\text{ext}} := \{e : \exists T \in \mathcal{T}_h : e = \partial T \cap \Gamma\},$$

respectively. For an interior face $e = \partial T_\alpha \cap \partial T_\beta$ with $\alpha < \beta$, the jump and the average values of an element–wise smooth function ϕ are defined as

$$[\![\phi]\!]_e := (\phi_{|T_\alpha})_{|e} - (\phi_{|T_\beta})_{|e} \quad \text{and} \quad \{\phi\}_e := \frac{1}{2}\Big((\phi_{|T_\alpha})_{|e} + (\phi_{|T_\beta})_{|e}\Big),$$

respectively, and the diameter of the face e is denoted by h_e.

For $s > \frac{3}{2}$ we introduce the broken Sobolev space

$$\mathcal{V} := \big\{v \in L^2(\Omega) : v_{|T} \in H^s(T) \quad \forall T \in \mathcal{T}_h\big\},$$

and the semi–discrete bilinear form for $u, v \in \mathcal{V}$

$$a_{DG}(u,v) := \sum_{T\in\mathcal{T}_h} \int_T \nabla u(x)\cdot\nabla v(x)\,dx - \sum_{e\in\mathcal{E}_h^{\text{int}}} \int_{\partial T_e} \{n\cdot\nabla u\}_e(x)\,[\![v]\!]_e(x)\,ds_x \tag{2.8}$$

$$-\xi \sum_{e\in\mathcal{E}_h^{\text{int}}} \int_{\partial T_e} \{n\cdot\nabla v\}_e(x)\,[\![u]\!]_e(x)\,ds_x + \sum_{e\in\mathcal{E}_h^{int}} \int_{\partial T_e} \frac{\sigma_e}{h_e} \int_e [\![u]\!]_e(x)\,[\![v]\!]_e(x)\,ds_x,$$

where ξ is a formulation parameter. In particular, the values $\xi \in \{-1, 0, 1\}$ correspond to non–symmetric, incomplete, and symmetric interior penalty DG finite element methods, respectively. The parameters $\sigma_e > 0$ are required for stabilization. The related energy norm is given by

$$\|v\|_{DG}^2 := \sum_{T\in\mathcal{T}_h} \|\nabla v\|_{L^2(T)}^2 + \sum_{e\in\mathcal{E}_h^{\text{int}}} \frac{\sigma_e}{h_e} \|[\![v]\!]\|_{L^2(e)}^2. \tag{2.9}$$

Let

$$\mathcal{V}_h := \big\{v_h \in L^2(\Omega) : v_{h|T} \in \mathbb{P}_p(T) \quad \forall T \in \mathcal{T}_h\big\} = \text{span}\{\varphi_i\}_{i=1}^M \tag{2.10}$$

denote the standard finite element space of local polynomials of degree p. For the coupling with boundary element methods it is useful to consider a splitting of $\mathcal{V}_h = \mathcal{V}_h^\Omega \oplus \mathcal{V}_h^\Gamma$ with

$$\mathcal{V}_h^\Omega = \text{span}\{\varphi_i : \varphi_{i|\Gamma} = 0\}_{i=1}^{M_\Omega} \quad \text{and} \quad \mathcal{V}_h^\Gamma = \text{span}\{\varphi_i\}_{i=M_\Omega+1}^{M}, \tag{2.11}$$

where ℓ refers to the refinement level, and $h_\ell = 2h_{\ell+1}$.

Table 1 contains numerical results for six meshes (five refinement levels) for all three schemes. Clearly the results support the notion that the asymptotic order of convergence is linear. Table 2 mimics Table 1 except it is based on the L_2–norm

$$e_2(h) = \|u_i - u_{i,h}\|_{L_2(\Omega)}$$

rather than the energy norm. As expected, the asymptotic order of convergence is quadratic.

			Galerkin (3.18)		Galerkin (3.19)		Collocation (3.20)	
N_Ω	N_Γ	M_Γ	$\widehat{e}_{DG}$	eoc	$\widehat{e}_{DG}$	eoc	$\widehat{e}_{DG}$	eoc
181	122	63	0.97194		0.97367		0.97142	
1448	488	246	0.54862	0.83	0.54885	0.83	0.54836	0.82
11584	1952	978	0.30130	0.86	0.30133	0.87	0.30122	0.86
92672	7808	3906	0.15793	0.93	0.15794	0.93	0.15792	0.93
741376	31232	15618	0.08048	0.97	0.08049	0.97	0.08049	0.97
5931008	124928	62466	0.04051	0.99	0.04053	0.99	0.04053	0.99

Table 1: Errors and rates of convergence for the third method measured using the energy norm.

			Galerkin (3.18)		Galerkin (3.19)		Collocation (3.20)	
N_Ω	N_Γ	M_Γ	e_2	eoc	e_2	eoc	e_2	eoc
181	122	63	0.130635		0.131305		0.130192	
1448	488	246	0.043916	1.57	0.044012	1.58	0.043716	1.57
11584	1952	978	0.014988	1.55	0.015001	1.55	0.014937	1.55
92672	7808	3906	0.004495	1.74	0.004501	1.74	0.004487	1.74
741376	31232	15618	0.001224	1.88	0.001231	1.87	0.001228	1.87
5931008	124928	62466	0.000319	1.98	0.000319	1.95	0.000319	1.95

Table 2: Errors and rates of convergence for the third method measured using the L_2–norm.

Numerical results for the three–field formulation (3.7)–(3.9) are given in Table 3, where we use the DG energy norm

$$e_{DG}(h) := \|u_i - u_{i,h}\|_{DG}$$

and the L_2–norm. Again we observe the expected linear and quadratic orders of convergence, respectively.

Finally, Table 4 contains numerical results for the non–symmetric approach (3.1)–(3.2) for the Galerkin (3.5) and collocation (3.6) schemes.

Numerical results indicate that all versions of the three methods performed similarly to each other. In particular, all of them exhibit linear order of convergence in the pertinent

5. Numerical Examples

In this section, we present numerical results confirming the theoretical results established for the third method and suggesting that the first two methods are stable and exhibit expected rates of convergence in the energy and L_2–norms.

In all examples, Ω is a unit sphere, and

$$f(x) = \widetilde{f}(r,\phi,\theta) = 4(\cos\phi + \sin\phi)\sin\theta\,,$$

where r,ϕ,θ are the spherical coordinates whose origin is at the sphere center. The exact solution for this problem is

$$u(x) = \widetilde{u}(r,\phi,\theta) = \frac{1}{3}(\cos\phi+\sin\phi)\sin\theta \cdot \begin{cases} (4-3r)r & \text{for } r<1, \\ r^{-2} & \text{for } r>1. \end{cases}$$

This function is piecewise analytic, and therefore the numerical solutions are expected to have the optimal rates of convergence.

Numerical solutions were obtained using piecewise linear discontinuous finite element basis functions for $\mathcal{V}_h$, piecewise linear continuous basis functions for $\mathcal{Q}_h$, and piecewise constant basis functions for $\mathcal{W}_h$. The interface Γ was approximated using piecewise linear continuous basis functions; errors associated with this approximation can be estimated and controlled by using standard techniques, e.g. [5, 15]. The collocation and Galerkin boundary element methods were accelerated using the fast multipole method; again the errors associated with the use of multipole and local expansions were estimated and controlled following [18]. The DG formulation parameters were chosen to be $\xi = \eta = 1$, and the DG stabilisation parameters were chosen to be $\sigma_e = 5$.

In presenting results, we denote the number of finite elements T in Ω by N_Ω, the number of elements on Γ by N_Γ, and the number of nodes on Γ by M_Γ.

First, let us present numerical results for the third method (3.15)–(3.16) in which the exterior Steklov–Poincaré operator is discretized using either the symmetric Galerkin scheme (3.18), or the non–symmetric Galerkin scheme (3.19), or the non–symmetric collocation scheme (3.20). In all cases, the error norm was computed as the modified energy norm

$$\begin{aligned}[\widehat{e}_{DG}(h)]^2 \;:=\; & \sum_{T\in\mathcal{T}_h} \|\nabla(u_i-u_{i,h})\|^2_{L^2(T)} + \sum_{e\in\mathcal{E}_h^{\rm int}} \frac{\sigma_e}{h_e}\|[\![u_i-u_{i,h}]\!]\|^2_{L^2(e)} \\ & + \sum_{e\in\mathcal{E}_h^{\rm ext}} \frac{\sigma_e}{h_e}\|(u_i-u_{i,h})-(u_e-u_{e,h})\|^2_{L^2(e)} + \sum_{e\in\mathcal{E}_h^{\rm ext}} \frac{1}{h_e}\|u_e-u_{e,h}\|^2_{L_2(e)}\end{aligned}$$

where the $H^{1/2}(\Gamma)$–norm in (4.2) was replaced by a weighted $L_2(\Gamma)$–norm, e.g. [4]. The estimated order of convergence was computed as

$$\text{eoc} := \log_2\left(\frac{\widehat{e}_{DG}(h_\ell)}{\widehat{e}_{DG}(h_{\ell+1})}\right),$$

where $\mathcal{V}^\Omega$ is the space spanned by the degrees of freedom in the interior of Ω, and $\mathcal{V}_h^\Gamma$ is the space spanned by the degrees of freedom on the interface Γ. In addition, let

$$\widetilde{\mathcal{V}}_h^\Gamma = \text{span}\,\{\widetilde{\varphi}_i\}_{M_\Omega+1}^{\widetilde{M}} \subset \mathcal{V}_h^\Gamma$$

be the subspace of boundary basis functions continuous on Γ.

2.3. Coupling Methods

In this section, we briefly describe the coupling method of Gatica, Heuer, and Sayas [8]. We regard this method as the current state of the art for coupling DG finite element and boundary element methods. To this end, we consider the interior Neumann boundary value problem

$$-\Delta u_i(x) = f(x) \quad \text{for } x\in\Omega, \qquad \frac{\partial}{\partial n_x}u_i(x) = t_i(x) \quad \text{for } x\in\Gamma.$$

In the context of the interior penalty methods, this problem results in the variational problem of finding $u_{i,h}\in\mathcal{V}_h$ such that

$$a_{DG}(u_{i,h},v_h) = \int_\Omega f(x)v_h(x)dx + \int_\Gamma t_i(x)v_h(x)ds_x \quad \text{for all } v_h\in\mathcal{V}_h. \tag{2.12}$$

By using the Neumann transmission condition, $t_i = t_e$, and the Dirichlet to Neumann map (2.6), $t_e = -S^{\rm ext}u_e$, we obtain

$$a_{DG}(u_{i,h},v_h) + \langle S^{\rm ext}u_e, v_h\rangle_\Gamma = \langle f, v_h\rangle_\Omega, \quad u_i = u_e.$$

As in the symmetric coupling of classical finite element and boundary element methods [6, 23], we use the symmetric representation (2.6) of the Steklov–Poincaré operator $S^{\rm ext}$ to obtain

$$a_{DG}(u_{i,h},v_h) + \langle Du_e, v_h\rangle_\Gamma - \langle(\frac{1}{2}I - K')t_e, v_h\rangle_\Gamma = \langle f, v_h\rangle_\Omega \tag{2.13}$$

where

$$t_e = -V^{-1}(\frac{1}{2}I - K)u_e \in H^{-1/2}(\Gamma)$$

is the unique solution of the variational problem

$$\langle Vt_e, w\rangle_\Gamma + \langle(\frac{1}{2}I-K)u_e, w\rangle_\Gamma = 0 \quad \text{for all } w\in H^{-1/2}(\Gamma). \tag{2.14}$$

For a Galerkin discretization of the variational problem (2.13) and (2.14), we introduce a finite–dimensional ansatz space

$$\mathcal{W}_h = \text{span}\{\psi_k\}_{k=1}^{N_\Gamma} \subset H^{-1/2}(\Gamma),$$

and approximate u_e by the Dirichlet trace of $u_{i,h}$ on Γ. This results in the variational problem of finding $(u_{i,h}, t_{e,h}) \in (\mathcal{V}_h^\Omega \oplus \widetilde{\mathcal{V}}_h^\Gamma) \times \mathcal{W}_h$ such that

$$a_{DG}(u_{i,h}, v_h) + \langle Du_{i,h}, v_h\rangle_\Gamma - \langle (\frac{1}{2}I - K')t_{e,h}, v_h\rangle_\Gamma = \langle f, v_h\rangle_\Omega \tag{2.15}$$

for all $v_h \in \mathcal{V}_h^\Omega \oplus \widetilde{\mathcal{V}}_h^\Gamma$, and

$$\langle Vt_{e,h}, w_h\rangle_\Gamma + \langle (\frac{1}{2}I - K)u_{i,h}, w_h\rangle_\Gamma = 0 \quad \text{for all } w_h \in \mathcal{W}_h. \tag{2.16}$$

This variational problem was first proposed and analyzed in [8]. Since the hypersingular operator D requires the use of continuous basis functions, one must use the subspace $\mathcal{V}_h^\Omega \oplus \widetilde{\mathcal{V}}_h^\Gamma$ instead of the general space $\mathcal{V}_h$. Although this restriction guarantees unique solvability and leads to optimal error estimates, it is incompatible with the spirit of DG finite element methods. Furthermore, constructing the restricted subspace poses significant practical difficulties, especially for three-dimensional problems, and therefore the entire approach may not be appealing to practitioners. This issue may be addressed by introducing additional Lagrange multipliers that ensure continuity of u_h on Γ [8]. However, this modification seems to be also cumbersome for three-dimensional problems.

The variational problem (2.15)–(2.16) is equivalent to the system of linear algebraic equations

$$\begin{pmatrix} K_{\Omega\Omega}^{\mathrm{DG}} & \widetilde{K}_{\Gamma\Omega}^{\mathrm{DG}} & \\ \widetilde{K}_{\Omega\Gamma}^{\mathrm{DG}} & \widetilde{K}_{\Gamma\Gamma}^{\mathrm{DG}} + \widetilde{D}_h & -(\frac{1}{2}\widetilde{M}_h^\top - \widetilde{K}_h^\top) \\ & \frac{1}{2}\widetilde{M}_h - \widetilde{K}_h & V_h \end{pmatrix} \begin{pmatrix} \underline{u}_i^\Omega \\ \underline{u}_i^\Gamma \\ \underline{t}_e \end{pmatrix} = \begin{pmatrix} \underline{f}^\Omega \\ \underline{f}^\Gamma \\ \underline{0} \end{pmatrix}, \tag{2.17}$$

where

$$\begin{aligned}
K_{\Omega\Omega}^{\mathrm{DG}}[j,i] &= a_{DG}(\varphi_i, \varphi_j) && \text{for } i,j = 1,\ldots,M_\Omega,\\
\widetilde{K}_{\Gamma\Omega}^{\mathrm{DG}}[j,i] &= a_{DG}(\widetilde{\varphi}_{M_\Omega+i}, \varphi_j) && \text{for } i = 1,\ldots,\widetilde{M} - M_\Omega, j = 1,\ldots,M_\Omega,\\
\widetilde{K}_{\Omega\Gamma}^{\mathrm{DG}}[j,i] &= a_{DG}(\varphi_i, \widetilde{\varphi}_{M_\Omega+j}) && \text{for } i = 1,\ldots,M_\Omega, j = 1,\ldots,\widetilde{M} - M_\Omega,\\
\widetilde{K}_{\Gamma\Gamma}^{\mathrm{DG}}[j,i] &= a_{DG}(\widetilde{\varphi}_{M_\Omega+i}, \widetilde{\varphi}_{M_\Omega+j}) && \text{for } i,j = 1,\ldots,\widetilde{M} - M_\Omega
\end{aligned}$$

are the blocks of the DG finite element matrix. Further,

$$\begin{aligned}
\widetilde{D}_h[j,i] &= \langle D\widetilde{\varphi}_{M_\Omega+i}, \widetilde{\varphi}_{M_\Omega+j}\rangle_\Gamma, & \widetilde{M}_h[\ell,i] &= \langle \widetilde{\varphi}_{M_\Omega+i}, \psi_\ell\rangle_\Gamma,\\
V_h[\ell,k] &= \langle V\psi_k, \psi_\ell\rangle_\Gamma, & \widetilde{K}_h[\ell,i] &= \langle K\widetilde{\varphi}_{M_\Omega+i}, \psi_\ell\rangle_\Gamma,
\end{aligned}$$

for $i,j = 1,\ldots,\widetilde{M} - M_\Omega$, $k,\ell = 1,\ldots,N_\Gamma$ are the Galerkin boundary element matrices, and the right hand side is given by

$$\begin{aligned}
f_j^\Omega &= \int_\Omega f(x)\varphi_j(x)dx \quad \text{for } j = 1,\ldots,M_\Omega,\\
f_j^\Gamma &= \int_\Omega f(x)\varphi_{M_\Omega+j}(x)dx \quad \text{for all } j = 1,\ldots,\widetilde{M} - M_\Omega.
\end{aligned}$$

Theorem 4.3 *Let (u_i, u_e) be the weak solution of the model boundary value problem (2.1)–(2.3) such that $u_i \in H^s(\Omega)$ with $s > \frac{3}{2}$. Let $(u_{i,h}, u_{e,h})$ be the unique solution of the variational problem (3.15) and (3.16), and let $\widetilde{S}$ satisfy the approximation property*

$$\|(\widetilde{S} - S^{ext})u_e\|_{H^{-1/2}(\Gamma)} \le c_S \inf_{w_h \in \mathcal{W}_h} \|t_e - w_h\|_{H^{-1/2}(\Gamma)} \quad \text{with} \quad t_e = S^{ext}u_e. \tag{4.7}$$

Then there exists a constant $C > 0$ such that the quasi–optimal error estimate

$$\begin{aligned}
&\|(u_i - u_{i,h}, u_e - u_{e,h})\|_{\mathcal{A}}^2\\
&\le C \left[\|u_e - q_h\|_{H^{1/2}(\Gamma)}^2 + \|u_i - v_h\|_{DG}^2 + \sum_{e \in \mathcal{E}_h^{ext}} h_e \|\nabla(u_i - v_h)\cdot n\|_{L^2(e)}^2 \right.\\
&\qquad \left. + \sum_{e \in \mathcal{E}_h^{ext}} \frac{1+\sigma_e}{h_e} \|(u_i - v_h) - (u_e - q_h)\|_{L^2(e)}^2 + c_S \inf_{\tau_h \in \mathcal{W}_h} \|t_e - w_h\|_{H^{-1/2}(\Gamma)}^2 \right].
\end{aligned}$$

holds for all $(v_h, q_h) \in \mathcal{V}_h \times \mathcal{Q}_h$.

Proof. See Appendix. ∎

Remark 4.2 *The approximation property (4.7) holds unconditionally for the Galerkin approximations (3.18) and (3.19) [23, 24]. In contrast, for the collocation approximation (3.20), (4.7) holds if the approximation is stable. At present, stability of the approximation under general conditions is an open problem.*

Corollary 4.4 *Let all assumptions of Theorem 4.3 hold, and in addition $3/2 < s \le 2$. If $\mathcal{V}_h$ is the space of discontinuous linear finite element functions, $\mathcal{Q}_h$ is the space of piecewise continuous linear boundary element basis functions, and $\mathcal{W}_h$ is the space of piecewise constant boundary element basis functions, then there exists a constant $\overline{C}$ such that*

$$\|(u_i - u_{i,h}, u_e - u_{e,h})\|_{\mathcal{A}} \le \overline{C}\, h^{s-1} \left[\|u_i\|_{H^s(\Omega)} + |t_i|_{H^{s-3/2}(\Gamma)} \right]. \tag{4.8}$$

Remark 4.3 *Of course if $u_i \in H^2(\Omega)$, the error estimate implies linear convergence rate. This result is straightforward to generalize to approximations based on higher order polynomial basis functions. Such approximations are meaningful for sufficiently large s only.*

Remark 4.4 *The Schur complement systems (2.18), (3.4), (3.11) and of (3.21) allow for a unified treatment of the coupling methods. In particular, this unified structure allows one to exploit standard results pertaining to stability and error analysis. However, stability analysis of the non–symmetric formulation (3.1)–(3.2) requires additional considerations. While it is likely that a successful treatment of the non–symmetric formulation is possible along the lines proposed in [22, 25], it is not pursued in this paper. Here, we limit our study of this issue to presenting numerical results confirming expected theoretical results.*

which implies the estimate

$$\begin{aligned}\mathcal{A}(v_h,q_h;v_h,q_h) &\geq \left(c_1^A-\frac{1-\eta}{8}\right)\left(\sum_{T\in\mathcal{T}_h}\|\nabla v_h\|^2_{L^2(T)}+\sum_{e\in\mathcal{E}_h^{\rm int}}\frac{\sigma_e}{h_e}\|[\![v_h]\!]\|^2_{L^2(e)}\right)\\ &\quad+\left(1-\frac{1-\eta}{8}\right)\sum_{e\in\mathcal{E}_h^{\rm ext}}\frac{\sigma_e}{h_e}\|v_h-q_h\|^2_{L^2(e)}+c_1^{\widetilde{S}}\|q_h\|^2_{H^{1/2}(\Gamma)}\\ &\geq \min\left\{\left(1-\frac{1-\eta}{8}\right),\left(c_1^A-\frac{1-\eta}{8}\right),c_1^{\widetilde{S}}\right\}\|(v_h,q_h)\|^2_{\mathcal{A}}.\end{aligned}$$

Thus $\mathcal{A}(v_h,q_h;v_h,q_h)$ is elliptic for $\eta\in\{-1,0,1\}$, if we choose σ_e sufficiently large to ensure

$$c_1^A-\frac{1-\eta}{8}>0.$$

■

Remark 4.1 *If $\widetilde{S}$ corresponds to the symmetric Galerkin approximation (3.18), then the stability estimate (4.3) holds for any pair of boundary element spaces $\mathcal{Q}_h$ and $\mathcal{W}_h$, e.g. [23]. For the non–symmetric approximations (3.19) and (3.20), an additional stability condition becomes necessary. That condition requires properly chosen boundary element spaces $\mathcal{Q}_h$ and $\mathcal{W}_h$. In particular, this can be achieved by constructing $\mathcal{W}_h$ on a finer mesh in comparison to that used for constructing $\mathcal{Q}_h$, e.g. [26].*

Lemma 4.2 *Let (u_i,u_e) be the weak solution of the model boundary value problem (2.1)–(2.3) such that $u_i\in H^s(\Omega)$ with $s>\frac{3}{2}$ and $(u_{i,h},u_{e,h})$ be a solution of the variational problem (3.15) and (3.16). Then the perturbed Galerkin orthogonality condition takes the form*

$$\mathcal{A}(u_i-u_{i,h},u_e-u_{e,h};v_h,q_h)=\langle(\widetilde{S}-S^{ext})u_e,q_h\rangle_\Gamma\quad \textit{for all } \mathcal{V}_h\times\mathcal{Q}_h. \tag{4.6}$$

Proof. Theorem 3.2 in [10] implies

$$\widehat{a}_{DG}(u_i,v)-\eta\langle n\cdot\nabla v,u_e\rangle_\Gamma-\sum_{e\in\mathcal{E}_h^{\rm ext}}\frac{\sigma_e}{h_e}\int_e u_e v ds_x=\langle f,v\rangle_\Gamma\quad\text{for all } v\in\mathcal{V}\,.$$

The solution (u_i,u_e) satisfies

$$\langle S^{\rm ext}u_e,q\rangle_\Gamma+\langle n\cdot\nabla u_i,q\rangle_\Gamma+\sum_{e\in\mathcal{E}_h^{\rm ext}}\frac{\sigma_e}{h_e}\int_e[u_e-u_i]q ds_x=0\quad\text{for all } q\in H^{1/2}(\Gamma).$$

Hence we conclude that

$$\mathcal{A}(u_i,u_e;v,q)+\langle(S^{\rm ext}-\widetilde{S})u_e,q,\rangle_\Gamma=\langle f,v\rangle_\Omega\quad\text{for all } (v,q)\in\mathcal{V}\times H^{1/2}(\Gamma).$$

The solution $(u_{i,h},u_{e,h})$ satisfies

$$\mathcal{A}(u_{i,h},u_{e,h};v_h,q_h)=\langle f,v_h\rangle_\Omega\quad\text{for all } (v_h,q_h)\in\mathcal{V}_h\times\mathcal{Q}_h.$$

For a conforming approach, $\mathcal{V}_h\times\mathcal{Q}_h\subset\mathcal{V}\times H^{1/2}(\Gamma)$, the last two equations imply (4.6). ■

Since the discrete single layer integral operator V_h is symmetric and positive definite, we can eliminate the discrete exterior Neumann datum $\underline{t}_e$ to obtain the Schur complement system

$$\begin{pmatrix} K_{\Omega\Omega}^{\rm DG} & \widetilde{K}_{\Gamma\Omega}^{\rm DG}\\ \widetilde{K}_{\Omega\Gamma}^{\rm DG} & \widetilde{K}_{\Gamma\Gamma}^{\rm DG}+\widetilde{S}_h^{\rm sym}\end{pmatrix}\begin{pmatrix}\underline{u}_i^\Omega\\ \underline{u}_i^\Gamma\end{pmatrix}=\begin{pmatrix}\underline{f}^\Omega\\ \underline{f}^\Gamma\end{pmatrix}, \tag{2.18}$$

where

$$\widetilde{S}_h^{\rm sym}=\widetilde{D}_h+(\frac{1}{2}\widetilde{M}_h^\top-\widetilde{K}_h^\top)V_h^{-1}(\frac{1}{2}\widetilde{M}_h-\widetilde{K}_h) \tag{2.19}$$

is a symmetric Galerkin boundary element approximation of the exterior Steklov–Poincaré operator (2.6). Note that $\widetilde{S}_h^{\rm sym}$ is positive definite for any choice of admissible basis functions $\widetilde{\varphi}_i$ and ψ_k, e.g. [23].

3. New Coupling Methods

In this section, we present three new coupling methods for the interior penalty DG finite element methods and boundary element methods. All three methods allow one to use the standard space $\mathcal{V}_h$ of globally discontinuous finite element functions, which significantly simplifies the implementation in comparison to the coupling methods that require functions continuous on Γ. Some of the coupling methods admit both collocation and Galerkin boundary element methods, which is particularly useful for practitioners.

3.1. First Method: Non–Symmetric Coupling

This method simply extends Johnson–Nédélec's coupling method [13] involving classical finite element methods to DG finite element methods. This method uses only the first integral equation in (2.5), and therefore the corresponding Steklov–Poincaré operator is represented as

$$t_e=-S^{\rm ext}u_e=-V^{-1}(\frac{1}{2}I-K)u_e.$$

By combining this equation with the Dirichlet transmission condition $u_i=u_e$, we obtain the variational problem of finding $(u_{i,h},t_{e,h})\in\mathcal{V}_h\times\mathcal{W}_h$ such that

$$\begin{aligned} a_{DG}(u_{i,h},v_h)-\langle t_{e,h},v_h\rangle_\Gamma &= \langle f,v_h\rangle_\Omega\quad\text{for all } v_h\in\mathcal{V}_h, &(3.1)\\ \langle Vt_{e,h},w_h\rangle_\Gamma+\langle(\frac{1}{2}I-K)u_{i,h},w_h\rangle_\Gamma &= 0\quad\text{for all } w_h\in\mathcal{W}_h. &(3.2)\end{aligned}$$

Since the hypersingular operator D does not appear in these equations, we can solve them using the standard discontinuous finite element space $\mathcal{V}_h$.

The variational problem (3.1) and (3.2) is equivalent to the system of linear algebraic equations

$$\begin{pmatrix} K^{\rm DG}_{\Omega\Omega} & K^{\rm DG}_{\Gamma\Omega} & \\ K^{\rm DG}_{\Omega\Gamma} & K^{\rm DG}_{\Gamma\Gamma} & -\widehat{M}_h^\top \\ & \frac{1}{2}\widehat{M}_h - \widehat{K}_h & V_h \end{pmatrix} \begin{pmatrix} \underline{u}_i^\Omega \\ \underline{u}_i^\Gamma \\ \underline{t}_e \end{pmatrix} = \begin{pmatrix} \underline{f}^\Omega \\ \underline{f}^\Gamma \\ \underline{0} \end{pmatrix}, \tag{3.3}$$

where

$$K^{\rm DG}[j,i] = a_{DG}(\varphi_i, \varphi_j), \quad f_j = \langle f, \varphi_j\rangle_\Omega \quad \text{for } i,j = 1,\ldots,M.$$

The blocks of the stiffness matrix and the right hand side vector are obtained according to the splitting (2.11). The blocks

$$\widehat{M}_h[\ell,i] = \langle \varphi_{M_\Omega+i}, \psi_\ell\rangle_\Gamma \quad \text{and} \quad \widehat{K}_h[\ell,i] = \langle K\varphi_{M_\Omega+i}, \psi_\ell\rangle_\Gamma$$

for $i = 1,\ldots,M-M_\Omega, \ell = 1,\ldots,N_\Gamma$, and the block V_h has been already introduced in (2.17). This system of linear algebraic equations does not have any apparent symmetry properties.

By eliminating the discrete Neumann datum $\underline{t}_e$ we obtain the Schur complement system

$$\begin{pmatrix} K^{\rm DG}_{\Omega\Omega} & K^{\rm DG}_{\Gamma\Omega} \\ K^{\rm DG}_{\Omega\Gamma} & K^{\rm DG}_{\Gamma\Gamma} + \widehat{S}_h^{\rm ns,G} \end{pmatrix} \begin{pmatrix} \underline{u}_i^\Omega \\ \underline{u}_i^\Gamma \end{pmatrix} = \begin{pmatrix} \underline{f}^\Omega \\ \underline{f}^\Gamma \end{pmatrix}, \tag{3.4}$$

where

$$\widehat{S}_h^{\rm ns,G} = \widehat{M}_h^\top V_h^{-1}(\frac{1}{2}\widehat{M}_h - \widehat{K}_h) \tag{3.5}$$

is a non–symmetric Galerkin boundary element approximation of the exterior Steklov–Poincaré operator (2.6).

In contrast to the symmetric approximation (2.19), $\widehat{S}_h^{\rm ns,G}$ is in general not positive definite, and therefore a certain stability condition is necessary for positive definiteness. That condition can be satisfied with a proper choice of the basis functions $\varphi_{i|\Gamma}$ and ψ_k, e.g. [23, 26]. The stability condition is not necessary when the coupling involves classical finite element methods [22, 25]. In this paper, we simply conjecture that the stability condition is also not necessary when the coupling involves DG finite element methods. In Section 5, we present numerical examples supporting this conjecture.

The singular boundary integral equation also admits collocation discretizations. This results in the approximate Steklov–Poincaré operator

$$\widehat{S}_h^{\rm ns,C} = \widehat{M}_h^\top \overline{V}_h^{-1}(\frac{1}{2}\overline{M}_h - \overline{K}_h), \tag{3.6}$$

where

$$\overline{V}_h[\ell,k] = (V\psi_k)(x_\ell^*), \quad \overline{M}_h[\ell,i] = \varphi_{M_\Omega+i}(x_\ell^*), \quad \overline{K}_h[\ell,i] = (K\varphi_{M_\Omega+i})(x_\ell^*)$$

for $i = 1,\ldots,M-M_\Omega$, $\ell = 1,\ldots,N_\Gamma$ are the entries of the collocation matrices, and x_ℓ^* are collocation nodes.

Also we define the energy norm

$$\|(v,q)\|_{\mathcal{A}}^2 := \sum_{T\in\mathcal{T}_h} \|\nabla v\|^2_{L^2(T)} + \sum_{e\in\mathcal{E}_h^{\rm int}} \frac{\sigma_e}{h_e}\|[\![v]\!]\|^2_{L^2(e)} + \sum_{e\in\mathcal{E}_h^{\rm ext}} \frac{\sigma_e}{h_e}\|v-q\|^2_{L^2(e)} + \|q\|^2_{H^{1/2}(\Gamma)}. \tag{4.2}$$

Theorem 4.1 *Let $\widetilde{S}$ be a stable boundary element approximation of the exterior Steklov–Poincaré operator (2.6),*

$$\langle \widetilde{S}q_h, q_h\rangle_\Gamma \geq c_1^{\widetilde{S}}\|q_h\|^2_{H^{1/2}(\Gamma)} \quad \textit{for all } q_h \in \mathcal{Q}_h, \tag{4.3}$$

and $\eta \in \{-1,0,+1\}$. Then for sufficiently large stability parameters σ_e, the bilinear form (4.1) is elliptic,

$$\mathcal{A}(v_h,q_h;v_h,q_h) \geq c_1^{\mathcal{A}}\,\|(v_h,q_h)\|^2_{\mathcal{A}} \quad \textit{for all } (v_h,q_h)\in\mathcal{V}_h\times\mathcal{Q}_h\,, \tag{4.4}$$

and the variational problem (3.15)–(3.16) has a unique solution.

Proof. For sufficiently large σ_e, the bilinear form $a_{DG}(\cdot,\cdot)$ defined in (2.8) is elliptic [19]. That is, there exists a constant $c_1^A > 0$ independent of h such that

$$a_{DG}(v_h,v_h) \geq c_1^A\,\|v_h\|^2_{DG} \quad \text{for all } v_h\in\mathcal{V}_h, \tag{4.5}$$

where

$$\|v_h\|^2_{DG} := \sum_{T\in\mathcal{T}_h}\|\nabla v_h\|^2_{L^2(T)} + \sum_{e\in\mathcal{E}_h^{\rm int}}\frac{\sigma_e}{h_e}\|[\![v_h]\!]\|^2_{L^2(e)}.$$

By inserting (3.14) in (4.1) and using (4.3) and (4.5), we obtain the inequality

$$\begin{aligned}
\mathcal{A}(v_h,q_h;v_h,q_h) &= a_{DG}(v_h,v_h) + \langle\widetilde{S}q_h,q_h\rangle_\Gamma \\
&\quad -(1-\eta)\langle n\cdot\nabla v_h, v_h-q_h\rangle_\Gamma + \sum_{e\in\mathcal{E}_h^{\rm ext}}\frac{\sigma_e}{h_e}\int_e [v_h-q_h]^2 ds_x \\
&\geq c_1^A\|v_h\|^2_{DG} + c_1^{\widetilde{S}}\|q_h\|^2_{H^{1/2}(\Gamma)} \\
&\quad -(1-\eta)\,|\langle n\cdot\nabla v_h, v_h-q_h\rangle_\Gamma| + \sum_{e\in\mathcal{E}_h^{\rm ext}}\frac{\sigma_e}{h_e}\int_e [v_h-q_h]^2 ds_x\,.
\end{aligned}$$

One can show (see Remark 3.1 in [10]) that

$$|\langle v_h-q_h, n\cdot\nabla v_h\rangle_\Gamma| \leq \frac{1}{8}\sum_{T\in\mathcal{T}_h}\|\nabla v_h\|^2_{L^2(T)} + \frac{1}{8}\sum_{e\in\mathcal{E}_h^{\rm ext}}\frac{\sigma_e}{h_e}\|v_h-q_h\|^2_{L^2(e)},$$

for $i = 1, \ldots, M - M_\Omega, j = 1, \ldots, M_\Gamma$, and

$$C_h[j,i] = \sum_{e \in \mathcal{E}_h^{\rm ext}} \frac{\sigma_e}{h_e} \int_e \phi_i \, \phi_j \, ds_x \quad \text{for } i,j = 1, \ldots, M_\Gamma.$$

The matrix $\widetilde{S}_h$ can represent any of the following approximations of the exterior Steklov–Poincaré operator (2.6), namely either the symmetric Galerkin approximation

$$\widetilde{S}_h^{\rm sym,G} = D_h + (\frac{1}{2} M_h^\top - K_h^\top) V_h^{-1} (\frac{1}{2} M_h - K_h), \tag{3.18}$$

or the non–symmetric Galerkin approximation

$$\widetilde{S}_h^{\rm ns,G} = M_h^\top V_h^{-1} (\frac{1}{2} M_h - K_h), \tag{3.19}$$

or the non–symmetric collocation approximation

$$\widetilde{S}_h^{\rm ns,C} = M_h^\top \overline{V}_h^{-1} (\frac{1}{2} \overline{M}_h - \overline{K}_h). \tag{3.20}$$

The Schur complement form of (3.17) is

$$\begin{pmatrix} K_{\Omega\Omega}^{\rm DG} & K_{\Gamma\Omega}^{\rm DG} \\ K_{\Omega\Gamma}^{\rm DG} & K_{\Gamma\Gamma}^{\rm DG} + \widetilde{S}_h^{\rm Dirichlet} \end{pmatrix} \begin{pmatrix} \underline{u}_i^\Omega \\ \underline{u}_i^\Gamma \end{pmatrix} = \begin{pmatrix} \underline{f}^\Omega \\ \underline{f}^\Gamma \end{pmatrix}, \tag{3.21}$$

with the discrete representation of the exterior Steklov–Poincaré operator

$$\widetilde{S}_h^{\rm Dirichlet} = -B_{-\eta,h}^\top \left[\widetilde{S}_h + C_h \right]^{-1} B_{1,h} \, . \tag{3.22}$$

As before, the matrix $\widetilde{S}_h$ can be represented by either $\widetilde{S}_h^{\rm sym,G}$, or $\widetilde{S}_h^{\rm ns,G}$, or $\widetilde{S}_h^{\rm ns,C}$.

4. Stability and Error Analysis

In this section, we establish unique solvability and error estimates for the governing equation (3.15)–(3.16) of the third method, with the provision that the approximation $\widetilde{S}$ of the Steklov–Poincaré operator (2.6) is stable.

Let us associate the variational problem (3.15)–(3.16) with the bilinear form

$$\begin{aligned} \mathcal{A}(u_i, u_e; v, q) \;&=\; \widehat{a}_{DG}(u_i, v_i) - \eta \langle n \cdot \nabla v, u_e \rangle_\Gamma - \sum_{e \in \mathcal{E}_h^{\rm ext}} \frac{\sigma_e}{h_e} \int_e u_e v \, ds_x \\ &\quad + \langle \widetilde{S} u_e, q \rangle_\Gamma + \langle n \cdot \nabla u_i, q \rangle_\Gamma + \sum_{e \in \mathcal{E}_h^{\rm ext}} \frac{\sigma_e}{h_e} \int_e [u_e - u_i] q \, ds_x. \end{aligned} \tag{4.1}$$

3.2. Second Method: Symmetric Three–Field Approach

This method is based on coupling of the interior penalty DG finite element methods and symmetric boundary element methods. In contrast to the first method, this method involves both integral equations in (2.5). The advantage of this method is that its stability can be proved, and the resulting system of linear algebraic equations is block skew symmetric; this algebraic structure can be advantageously exploited. The drawback of the method is that it does not admit collocation schemes. The method has the structure similar to that of the three–field domain decomposition method of Brezzi and Marini [1].

Like in the first method, we combine the variational problem (2.12) with the Neumann transmission condition $t_i = t_e$:

$$a_{DG}(u_{i,h}, v_h) - \langle t_e, v_h \rangle_\Gamma = \langle f, v_h \rangle_\Omega \quad \text{for all } v_h \in \mathcal{V}_h.$$

In contrast to the first method, we insert the Dirichlet transmission condition $u_i = u_e$ into the first boundary integral equation in (2.5), but we do not use this equation to eliminate u_e:

$$u_i = u_e = (\frac{1}{2} I + K) u_e - V t_e \quad \text{on } \Gamma.$$

To close the system of governing equations, we use the hypersingular boundary integral equation

$$D u_e + (\frac{1}{2} I + K') t_e = 0 \quad \text{on } \Gamma.$$

To proceed further, we need to address the fact that the hypersingular operator D and the double layer operator $\frac{1}{2} I + K$ have non–trivial kernels. Therefore the exterior Dirichlet trace u_e is not uniquely determined by the two boundary integral equations. To this end we recall that both kernels coincide:

$$u_0(x) = 1, \quad (D u_0)(x) = \frac{1}{2} u_0(x) + (K u_0)(x) = 0 \quad \text{for } x \in \Gamma \text{ a.e.}$$

Accordingly, we introduce the scaling condition

$$\langle u_e, 1 \rangle_\Gamma = 0,$$

and the stabilized hypersingular operator D_s defined as [17]

$$\langle D_s u, v \rangle_\Gamma = \langle D u, v \rangle_\Gamma + \langle u, 1 \rangle_\Gamma \langle v, 1 \rangle_\Gamma \quad \text{for all } u, v \in H^{1/2}(\Gamma).$$

In addition to the trial space $\mathcal{V}_h$, we introduce an ansatz space

$$\mathcal{Q}_h = \operatorname{span}\{\phi_i\}_{i=1}^{M_\Gamma} \subset H^{1/2}(\Gamma) \cap C(\Gamma)$$

of continuous basis functions ϕ_i. As a result we arrive at the variational problem of finding $(u_{i,h}, t_{e,h}, u_{e,h}) \in \mathcal{V}_h \times \mathcal{W}_h \times \mathcal{Q}_h$ such that

$$\begin{aligned} a_{DG}(u_{i,h}, v_h) - \langle t_{e,h}, v_h\rangle_\Gamma &= \langle f, v_h\rangle_\Omega \text{ for all } v_h \in \mathcal{V}_h, && (3.7)\\ \langle u_{i,h}, w_h\rangle_\Gamma + \langle V t_{e,h}, w_h\rangle_\Gamma - \langle (\frac{1}{2}I + K)u_{e,h}, w_h\rangle_\Gamma &= 0 \quad \text{for all } w_h \in \mathcal{W}_h, && (3.8)\\ \langle (\frac{1}{2}I + K')t_{e,h}, q_h\rangle_\Gamma + \langle D_s u_{e,h}, q_h\rangle_\Gamma &= 0 \quad \text{for all } q_h \in \mathcal{Q}_h. && (3.9) \end{aligned}$$

This variational problem is equivalent to the system of linear algebraic equations

$$\begin{pmatrix} K_{\Omega\Omega}^{\rm DG} & K_{\Gamma\Omega}^{\rm DG} & & \\ K_{\Omega\Gamma}^{\rm DG} & K_{\Gamma\Gamma}^{\rm DG} & -\widehat{M}_h^\top & \\ & \widehat{M}_h & V_h & -\frac{1}{2}M_h - K_h \\ & & \frac{1}{2}M_h^\top + K_h^\top & D_{s,h} \end{pmatrix} \begin{pmatrix} \underline{u}_i^\Omega \\ \underline{u}_i^\Gamma \\ \underline{t}_e \\ \underline{u}_e \end{pmatrix} = \begin{pmatrix} \underline{f}^\Omega \\ \underline{f}^\Gamma \\ \underline{0} \\ \underline{0} \end{pmatrix}, \qquad (3.10)$$

where in addition to those block matrices already used in (3.3) we have

$$D_{s,h}[j,i] = \langle D_s\phi_i, \phi_j\rangle_\Gamma, \quad M_h[\ell,i] = \langle \phi_i, \psi_\ell\rangle_\Gamma, \quad K_h[\ell,i] = \langle K\phi_i, \psi_\ell\rangle_\Gamma$$

for $i,j = 1,\ldots,M_\Gamma$, $\ell = 1,\ldots,N_\Gamma$. By eliminating $\underline{u}_e$ and $\underline{t}_e$ from (3.10) we obtain the Schur complement system

$$\begin{pmatrix} K_{\Omega\Omega}^{\rm DG} & K_{\Gamma\Omega}^{\rm DG} \\ K_{\Omega\Gamma}^{\rm DG} & K_{\Gamma\Gamma}^{\rm DG} + S_h^{\rm three} \end{pmatrix} \begin{pmatrix} \underline{u}_i^\Omega \\ \underline{u}_i^\Gamma \end{pmatrix} = \begin{pmatrix} \underline{f}^\Omega \\ \underline{f}^\Gamma \end{pmatrix}, \qquad (3.11)$$

with the symmetric three–field approximation of the exterior Steklov–Poincaré operator

$$\widetilde{S}_h^{\rm three} = \widehat{M}_h^\top \left[V_h + (\frac{1}{2}M_h + K_h) D_{s,h}^{-1} (\frac{1}{2}M_h^\top + K_h) \right]^{-1} \widehat{M}_h. \qquad (3.12)$$

3.3. Third Method: Dirichlet Based Coupling

In the first two methods, the coupling involves passing the exterior Neumann data t_e to the variational problem for the interior boundary value problem. In contrast, in the third method, the coupling is based on the Dirichlet transmission condition $u_i = u_e$. This approach is similar to the coupling of DG and mixed finite element methods proposed by Girault, Sun, Wheeler, and Yotov [10].

The solution u_i of the model problem (2.1)–(2.3) coincides with the solution of the Dirichlet boundary value problem

$$-\Delta u_i = f \quad \text{in } \Omega, \quad u_i = u_e \quad \text{on } \Gamma.$$

Following [10], the discrete variational problem corresponding to this boundary value problem is to find $u_{i,h} \in \mathcal{V}_h$ such that for all $v_h \in \mathcal{V}_h$

$$\widehat{a}_{DG}(u_{i,h}, v_h) - \eta\langle u_e, \nabla v_h \cdot n\rangle_\Gamma - \sum_{e\in\mathcal{E}_h^{\rm ext}} \frac{\sigma_e}{h_e}\int_e u_e v_h ds = \langle f, v_h\rangle_\Omega, \qquad (3.13)$$

where

$$\widehat{a}_{DG}(u,v) := a_{DG}(u,v) - \langle n\cdot\nabla u, v\rangle_\Gamma + \eta\,\langle n\cdot\nabla v, u\rangle_\Gamma + \sum_{e\in\mathcal{E}_h^{\rm ext}} \frac{\sigma_e}{h_e}\int_e u\,v\,ds_x\,. \qquad (3.14)$$

Here $\eta \in \{-1, 0, +1\}$ is a formulation parameter, similar to the formulation parameter ξ in (2.8).

Let us combine the Dirichlet to Neumann map (2.6) and the Neumann transmission condition $t_e = t_i = n\cdot\nabla u_i$, so that we obtain

$$S^{\rm ext} u_e = -n\cdot\nabla u_i \quad \text{on } \Gamma.$$

By adding a stabilization term to this equation [10] and approximating u_e by a function $u_{e,h} \in \mathcal{Q}_h$, we obtain the variational problem of finding $(u_{i,h}, u_{e,h}) \in \mathcal{V}_h \times \mathcal{Q}_h$ such that

$$\widehat{a}_{DG}(u_{i,h}, v_h) - \eta\langle n\cdot\nabla v_h, u_{e,h}\rangle_\Gamma - \sum_{e\in\mathcal{E}_h^{\rm ext}} \frac{\sigma_e}{h_e}\int_e u_{e,h} v_h ds_x = \langle f, v_h\rangle_\Gamma \qquad (3.15)$$

for all $v_h \in \mathcal{V}_h$, and

$$\langle \widetilde{S} u_{e,h}, q_h\rangle_\Gamma + \langle n\cdot\nabla u_{i,h}, q_h\rangle_\Gamma + \sum_{e\in\mathcal{E}_h^{\rm ext}} \frac{\sigma_e}{h_e}\int_e [u_{e,h} - u_{i,h}] q_h ds_x = 0 \qquad (3.16)$$

for all $q_h \in \mathcal{Q}_h$, where $\widetilde{S}$ is a boundary element approximation of the exterior Steklov–Poincaré operator (2.6).

The variational problem (3.15)–(3.16) is equivalent to the system of linear algebraic equations

$$\begin{pmatrix} \widehat{K}_{\Omega\Omega}^{\rm DG} & \widehat{K}_{\Gamma\Omega}^{\rm DG} & \\ \widehat{K}_{\Omega\Gamma}^{\rm DG} & \widehat{K}_{\Gamma\Gamma}^{\rm DG} & B_{-\eta,h}^\top \\ & B_{1,h} & \widetilde{S}_h + C_h \end{pmatrix} \begin{pmatrix} \underline{u}_i^\Omega \\ \underline{u}_i^\Gamma \\ \underline{u}_e \end{pmatrix} = \begin{pmatrix} \underline{f}^\Omega \\ \underline{f}^\Gamma \\ \underline{0} \end{pmatrix}, \qquad (3.17)$$

where

$$\widehat{K}^{\rm DG}[j,i] = \widehat{a}_{DG}(\varphi_i, \varphi_j) \quad \text{for } i,j = 1,\ldots,M$$

is the stiffness matrix of the modified discontinous Galerkin finite element method which is obtained according to the splitting (2.11). Further,

$$B_{r,h}[j,i] = r\langle n\cdot\nabla\varphi_{M_\Omega+i}, \phi_j\rangle_\Gamma - \sum_{e\in\mathcal{E}_h^{\rm ext}} \frac{\sigma_e}{h_e}\int_e \varphi_{M_\Omega+i}\,\phi_j\,ds_x$$